Since January 2020 Elsevier has created a COVID-19 resource centre with free information in English and Mandarin on the novel coronavirus COVID-19. The COVID-19 resource centre is hosted on Elsevier Connect, the company's public news and information website.

Elsevier hereby grants permission to make all its COVID-19-related research that is available on the COVID-19 resource centre - including this research content - immediately available in PubMed Central and other publicly funded repositories, such as the WHO COVID database with rights for unrestricted research re-use and analyses in any form or by any means with acknowledgement of the original source. These permissions are granted for free by Elsevier for as long as the COVID-19 resource centre remains active.

Antiviral Research 177 (2020) 104714

Contents lists available at ScienceDirect

Antiviral Research

journal homepage: www.elsevier.com/locate/antiviral

Inhibition of herpes simplex virus by myricetin through targeting viral gD protein and cellular EGFR/PI3K/Akt pathway

Wenmiao Li[a,1], Cuijing Xu[a,1], Cui Hao[b,*], Yang Zhang[a], Zhaoqi Wang[a], Shuyao Wang[a], Wei Wang[a,c,**]

[a] Key Laboratory of Marine Drugs, Chinese Ministry of Education; School of Medicine and Pharmacy, Ocean University of China, Qingdao, 266003, PR China
[b] Systems Biology & Medicine Center for Complex Diseases, Affiliated Hospital of Qingdao University, Qingdao, 266003, PR China
[c] Laboratory for Marine Drugs and Bioproducts of Qingdao National Laboratory for Marine Science and Technology, Qingdao, 266237, PR China

ARTICLE INFO

Keywords:
Myricetin
Anti-HSV
Virus adsorption
Membrane fusion
EGFR/PI3K/Akt pathway

ABSTRACT

Myricetin, a common dietary flavonoid, was reported to possess many different biological activities such as antioxidant, anti-inflammatory, and antiviral effects. In this study, we explored the anti-HSV effects and mechanisms of myricetin both *in vitro* and *in vivo*. The results showed that myricetin possessed anti-HSV-1 and HSV-2 activities with very low toxicity, superior to the effects of acyclovir. Myricetin may block HSV infection through direct interaction with virus gD protein to interfere with virus adsorption and membrane fusion, which was different from the nucleoside analogues such as acyclovir. Myricetin also down-regulate the cellular EGFR/PI3K/Akt signaling pathway to further inhibit HSV infection and its subsequent replication. Most importantly, intraperitoneal therapy of myricetin markedly improved mice survival and reduced virus titers in both lungs and spinal cord. Therefore, the natural dietary flavonoid myricetin has potential to be developed into a novel anti-HSV agent targeting both virus gD protein and cellular EGFR/PI3K/Akt pathway.

1. Introduction

Herpes simplex virus type 1 (HSV-1) and type 2 (HSV-2) are enveloped double stranded DNA viruses belonging to *Herpesviridae* (Fatahzadeh and Schwartz, 2007). HSV infection causes skin lesions that are generally localized at the oral, nasal, and ocular level with HSV-1 infection, whereas with HSV-2, infections most commonly occur at genital-skin and mucosa sites (Liu and Cohen, 2015; Smith and Robinson, 2002). Approximately 60%–90% of the adult human population worldwide is sera-positive for HSV-1 (Carr et al., 2001). The current FDA approved antiviral agents for herpesviruses involve mainly nucleoside analogues, such as acyclovir (ACV) and pencyclovir, which mainly inhibit viral genome replication. Despite these successes, drug resistance, and side effects remain unresolved issues in the fight against HSV infections (Morfin and Thouvenot, 2003). Hence, the development of novel anti-HSV agents with active mechanisms different from nucleoside analogues is of high importance.

Myricetin (3,5,7-trihydroxy-2-(3,4,5-trihydroxyphenyl)-4-benzopyrone) is a common dietary flavonoid from plant sources such as vegetables, fruits, and tea, with antioxidant properties (Ong and Khoo, 1997; Ross and Kasum, 2002). Like other flavonoids, myricetin is reported to possess many different biological activities such as antimicrobial, anti-thrombotic, neuroprotective, and anti-inflammatory effects (Cushnie and Lamb, 2005; Dajas et al., 2003; Gupta et al., 2014; Ong and Khoo, 1997; Santhakumar et al., 2014; Semwal et al., 2016; Tian et al., 2010). Pasetto et al. reported that myricetin possessed anti-HIV-1 activities with low toxicity, and it mainly inhibited the activity of HIV reverse transcriptase (Pasetto et al., 2014). Lyu et al. found that some flavonoids such as myricetin and quercetinin showed moderate inhibitory effects against HSV-1 in Vero cells (Lyu et al., 2005). Yu and co-workers found that myricetin and scutellarein potently inhibited the SARS-CoV helicase protein *in vitro* by affecting the ATPase activity, suggesting that myricetin and scultellarein might serve as SARS-CoV chemical inhibitors (Yu et al., 2012). Thus, myricetin has the potential to be developed into a novel anti-viral agent.

To further correlate the anti-viral applications of myricetin with its underlying molecular mechanisms, the anti-HSV effects and mechanisms of myricetin were investigated both *in vitro* and *in vivo* in this study. The results showed that myricetin possessed anti-HSV-1 and HSV-2 activities with very low toxicity. Myricetin may block HSV

* Corresponding author.
** Corresponding author. Key Laboratory of Marine Drugs, Ministry of Education, Ocean University of China, Qingdao 266003, PR China.
E-mail addresses: haocuiqdfy@163.com (C. Hao), wwwakin@ouc.edu.cn (W. Wang).
[1] These authors contributed equally to this work.

https://doi.org/10.1016/j.antiviral.2020.104714
Received 5 October 2019; Received in revised form 23 December 2019; Accepted 20 January 2020
Available online 09 March 2020
0166-3542/ © 2020 Elsevier B.V. All rights reserved.

infection through direct interaction with virus gD protein to interfere with virus adsorption and membrane fusion. Moreover, intraperitoneal therapy of myricetin markedly improved mice survival and reduced virus titers in both lungs and spinal cord. Thus, myricetin merits further investigation as a novel anti-HSV agent in the future.

2. Material and methods

2.1. Reagents, cells and viruses

Myricetin (with purity > 95%) was purchased from Topscience Co., Ltd. (Shanghai, China). Acyclovir was purchased from Sigma Aldrich (St. Louis, MO, USA). Vero, HeLa and Hep-2 cells were routinely cultured in Dulbecco's modified Eagle's medium (DMEM) supplemented with 10% fetal bovine serum (ExCell Bio, China), penicillin (100 U/mL), and streptomycin (100 μg/mL) at 37 °C in 5% CO_2. HSV-1 strain F was purchased from ATCC (VR-734). HSV-2 strain 333 was obtained from Wuhan Institute of Virology, Chinese Academy of Sciences.

2.2. Cytopathic effect (CPE) inhibition assay

The antiviral activity was evaluated by the CPE inhibition assay (Dai et al., 2018). Briefly, Vero cells in 96-well plates were infected with HSV-1 or HSV-2 at a multiplicity of infection (MOI) of 0.1, and then treated with indicated concentrations of myricetin in triplicate after removal of virus inoculum. After 24 h incubation, the cells were fixed with 4% formaldehyde for 20 min at room temperature (RT). After removal of the formaldehyde, the cells were stained with 0.1% (w/v) crystal violet for 30 min at 37 °C. The plates were washed and dried, and the intensity of crystal violet staining for each well was measured at 570 nm. The concentration required for a test compound to reduce the CPE of HSV by 50% (IC_{50}) was determined.

2.3. Plaque reduction assay

HSV-1 or HSV-2 (50–100 PFU/well) was pre-incubated with or without myricetin for 60 min at 37 °C before infection. Then the virus-myricetin mixture was transferred to Vero cell monolayers in 6-well plates, and incubated at 37 °C for 1 h with gentle shaking every 15 min. After that, the inoculum was removed and each well was overlaid with 2 mL of agar overlay media containing 1.5% agarose, 100 U/ml penicillin, and 100 μg/ml streptomycin. The cells were then incubated at 37 °C until plaque sizes were adequate. Then the cells were fixed with 4% paraformaldehyde (PFA) and stained with 1% crystal violet for plaque counting.

2.4. Time-of-addition assay

Vero cells were infected with HSV-1 or HSV-2 (MOI = 1.0) under four different treatment conditions: i) Pretreatment of virus: myricetin (20 μM) pretreated HSV was added to Vero cells and incubated at 37 °C for 1 h. Then after adsorption, the virus innuculum containing myricetin was removed and the cells were overlaid with compound-free media. ii) Pretreatment of cells: Vero cells were pretreated with 20 μM of myricetin before HSV infection. iii) Adsorption: Vero cells were infected in media containing myricetin (20 μM) at 4 °C for 1 h. After that, the virus innuculum was removed and the compound-free media were added into cells. iv) Post-adsorption: after removal of unabsorbed virus, myricetin (20 μM) was added to the cells. At 24 h p.i., virus yields were determined by plaque assay.

2.5. Indirect immunofluorescence assay

The indirect immunofluorescence assay was performed as previously described (Wang et al., 2017). Briefly, for HSV binding assay, HSV-1 (MOI = 1.0) was adsorbed to HeLa cells for 2 h at 4 °C in the absence or presence of 20 μM myricetin before washing with PBS. For entry assay, HSV-1 (MOI = 1.0) was firstly adsorbed to HeLa cells at 4 °C for 2 h before washing with PBS. Then myricetin (20 μM) was added to cells and incubated at 37 °C for 1 h. After that, cells were treated with proteinase K to remove adsorbed but not internalized virus. Then the cells were washed with PBS and fixed with 4% paraformaldehyde for 20 min. Then cells were permeabilized using 0.5% (v/v) Triton X-100 in PBS for 5 min before incubated with 2% BSA for 1 h at 37 °C. After washing, cells were incubated consecutively with anti-ICP5 antibodies (1:100 dilutions) and DyLight 649®-conjugated secondary antibodies. Then the cell nucleus was stained with DAPI for 20 min before confocal imaging. Images were recorded using a Nikon confocal microscope, and analysed by ImageJ (NIH) version 1.33 u (USA).

2.6. Real-time RT-PCR assay

The total RNA was extracted from HSV infected Vero cells using an RNAiso™ Plus Kit (Takara, Japan), and analysed by using the One Step SYBR PrimeScript RT-PCR Kit (Takara, Japan). The primer pairs for HSV gD and cellular β-actin mRNA were listed as follows: gD mRNA, 5′-AGCATCCCGATCACTGTGTACTA-3′ and 5′-GCGATGGTCAGGTTGT ACGT-3'; Monkey β-actin mRNA, 5′-CTCCATCCTGGCCTCGCTGT-3′ and 5′-GCTGTCACCTTCACCGTTCC-3'. The real-time RT-PCR was performed at 42 °C 5 min, 95 °C 10 s, 40 cycles of 95 °C 5 s, 60 °C 34 s, followed by melting curve analysis, according to the instrument documentation (ABI PRISM 7500, Applied Biosystems, USA). All reactions were performed in triplicate and the results were normalized to β-actin. The relative amounts of HSV gD mRNA molecules were determined using the comparative ($2^{-\Delta\Delta CT}$) method, as previously described (Livak and Schmittgen, 2001).

2.7. DARTS assay

DARTS experiments for identifying the targets of myricetin were performed as previously reported (Lomenick et al., 2009). Briefly, HSV-1 (MOI = 1.0) infected Vero cells were lysed with NP-40 cell lysis buffer (Beyotime, Nantong, China) and treated with or without myricetin (60 μM) for 1 h at room temperature (RT) followed by digested with pronase (3 μg/ml) in reaction buffer (50 mM Tris-HCl (pH 8.0), 50 mM NaCl, 10 mM CaCl2) for 30 min at RT. The digestion was stopped by directly add 5 × SDS-PAGE loading buffer and inactivation by boiling. Protein samples were separated with 10% SDS-polyacrylamide gels and analysed by western blot with antibodies against HSV-1 gD, gB, gC, gH/gL proteins or cellular HVEM, nectin-1, actin, tubulin proteins as controls.

2.8. Surface plasmon resonance (SPR) assay

SPR assays were conducted on a SPR biosensor instrument GE BiacoreT200 (GE, USA). HSV-1 gD proteins (Biodragon, Beijing, China) were firstly immobilized onto the surface of a carboxymethylated dextran sensor chip (CM5) via amino group coupling as described previously (Geng et al., 2003). To assess real-time binding of myricetin to the gD proteins on CM5 chips, myricetin with different concentrations (10, 5, 2.5, 1.25, 0.625, 0.3125 μM) dissolved in DMSO, was injected over the sensor chip surface with gD immobilized within 2 min, followed by a 10-min wash with 1 × PBST buffer. The sensor chip surface was then regenerated by washing with NaOH (2 mM) for 30 s. All binding experiments were carried out at 25 °C with a constant flow rate of 2 μl/s PBS buffer. To correct for non-specific binding and bulk refractive index change, a blank channel without gD was used and run simultaneously for each experiment. Then, the BiacoreT200 SPR evaluation software was used to calculate the kinetic parameters, and the changes in mass due to the binding response were recorded as

resonance units (RU).

2.9. Western blot assay

After drug treatment, the cell lysate was separated by SDS-PAGE and transferred to nitrocellulose membrane. After being blocked in Tris-buffered saline (TBS) containing 0.1% Tween 20 (v/v) and 5% BSA (w/v) at RT for 2 h, the membranes were rinsed and incubated at 4 °C overnight with primary antibodies against phosphorylated or non-phosphorylated EGFR, PI3K, Akt antibodies, or anti-α-tubulin and GAPDH antibodies (Cell Signaling Technology, Danvers, USA) as control. The membranes were washed and incubated with AP-labeled secondary antibody (1:2000 dilutions) at RT for 2 h. The protein bands were then visualized by incubating with the developing solution (p-nitro blue tetrazolium chloride (NBT) and 5-bromo-4-chloro-3-indolyl phosphate toluidine (BCIP)) at RT for 30 min. The relative densities of proteins were all determined by using ImageJ (NIH) v.1.33 u (USA).

2.10. Cell fusion inhibition assay

The cell fusion inhibition assay was performed as described with modifications (Du et al., 2017). Monolayers of Vero cells grown in 6-well plates were infected with HSV-2 (MOI = 3.0) at 4 °C for 2 h. After removal of virus inoculum, compound free media were added to cells and incubated at 37 °C for 5 h. Then myricetin (30 or 15 μM) was added to cells, and incubated at 37 °C for another 2 h. After that, cells were fixed and detected with hematoxylin-eosin (HE) staining. The inhibition of syncytium formation was examined by light microscopy. The influence of myricetin on HSV glycoprotein expression during 5–7 h post infection was also evaluated by western blotting.

2.11. Molecular docking

Molecular docking was conducted in MOE v2014.09011 (MOE, 2014). The 2D structures of myricetin was drawn in ChemBioDraw 2014 and converted to 3D structure in MOE through energy minimization. The 3D structure of the protein gD was downloaded from RCSB Protein Data Bank (PDB ID: 4MYV). Prior to docking, the force field of AMBER10: EHT and the implicit solvation model of Reaction Field (R-field) were selected. MOE-Dock was used for molecular docking simulations of myricetin with gD. The docking workflow followed the “induced fit” protocol, in which the side chains of the receptor pocket were allowed to move according to ligand conformations, with a constraint on their positions. The weight used for tethering side chain atoms to their original positions was 10. For each ligand, all docked poses of which were ranked by London dG scoring first, then a force field refinement was carried out on the top 20 poses followed by a rescoring of GBVI/WSA dG. The conformations with the lowest free energies of binding were selected as the best (probable) binding modes. Molecular graphics were generated by PyMOL.

2.12. Animal experiments

All animal experiments were performed in accordance with the National Institutes of Health guide for the care and use of Laboratory animals and approved by the Institutional Animal Care and Use Committee at Ocean University of China. Three-week-old female BALB/c mice (average weight, 11.0 ± 2.0 g) were purchased from Beijing Vital River Laboratory Animal Technology Co., Ltd. (Beijing, China) and raised in a pathogen-free environment (23 ± 2 °C and 55% ± 5% humidity). Mice were randomly divided into five experimental groups (10 mice each). Mice were anaesthetized and infected via the intranasal route with 10^6 PFU of HSV-1 (F strain) in 50 μL of PBS. Four hours after inoculation, mice received intraperitoneally treatment of acyclovir (10 mg·kg-1), myricetin (2.5 or 5 mg·kg-1), or placebo, and the treatments were repeated once daily for five days.

Each day mice were weighed and monitored for signs of illness for 14 days, and those suffering a severe infection or having lost > 20% of their original body weight were euthanized. To determine virus titers in organs, mice were euthanized, and the lungs, brains and spinal cords were removed, homogenized and clarified by centrifugation on Day 4 after inoculation. Samples were assayed for virus titers by plaque assay and quantitative RT-PCR assay. Histopathological analysis was also performed using H&E staining on lung and brain samples collected on Day 4.

2.13. Statistical analysis

All data are representative of at least three independent experiments. Data are presented as means ± standard deviations (S.D.). Statistical significance was analysed using GraphPad Prism 7 software using oneway ANOVA with Turkey's test. P values < 0.05 were considered significant.

3. Results

3.1. Inhibition of HSV multiplication in vitro by myricetin

Myricetin is a member of the flavonoid class of polyphenolic compounds, with antioxidant properties, and its structure is shown in Fig. 1A. Herein, the anti-HSV effects and mechanisms of myricetin were investigated *in vitro*. The cytotoxicity of myricetin in Vero, Hep-2 and HeLa cells was firstly assessed by MTT assay (Livak and Schmittgen, 2001). The results showed that myricetin exhibited no significant cytotoxicity at the concentrations from 50 to 400 μM (Fig. 1B). The CC_{50} (50% Cytotoxicity Concentration) value for myricetin in Vero, Hep-2 and HeLa cells was about 1097.9 ± 71.2 μM, 964.6 ± 94.7 μM, and 1152.3 ± 165.1 μM, respectively (Table 1).

Myricetin was then assayed for its ability to inhibit HSV multiplication *in vitro* using CPE inhibition assay and plaque assay (Li et al., 2017, 2018). Briefly, HSV-1 (F strain) or HSV-2 (333 strain) (MOI = 0.1) was pretreated with myricetin (1.25, 2.5, 5, 10 μM) for 1 h at 37 °C before infection, then after adsorption, the media containing myricetin at indicated concentrations were added to cells. At 24 h p.i., the viral titers in the culture media were determined by plaque assay, and cell viability was measured by CPE inhibition assay. As shown in Fig. 1C, myricetin significantly reduced the virus titers of both HSV-1 and HSV-2 in Vero cells when used at the concentration > 1.25 μM ($p < 0.05$). CPE inhibition assay showed that the IC_{50} values of myricetin was about 2.2 ± 0.3 μM and 1.6 ± 0.5 μM for HSV-1 and HSV-2, respectively, and the selectivity index (CC_{50}/IC_{50}) for myricetin was about 498.6 and 685.6, respectively, superior to that of acyclovir (ACV) (SI = 131.8 and 84.1) (Table 1). Myricetin also inhibited HSV replication in Hep-2 and HeLa cells with SI > 150 (Table 1). In addition, the plaque reduction assay showed that pretreatment of HSV with myricetin at the concentrations of 1.25–20 μM significantly reduced the number of plaques in both HSV-1 and HSV-2 infected cells (Fig. 1D–F), suggesting that myricetin may be able to inactivate viral particles directly.

3.2. Influence of different treatment conditions of myricetin on HSV infection

The time-of-addition assay was performed to determine the stage(s) at which myricetin exerted its inhibition actions *in vitro* (Li et al., 2018). In brief, myricetin was added to Vero cells under four different conditions: pre-treatment of viruses, pre-treatment of cells, during virus adsorption, or after adsorption. Subsequently, the antiviral activity was determined by plaque assay. As shown in Fig. 2A, pretreatment of HSV-1 or HSV-2 with 20 μM myricetin for 1 h before infection significantly reduced the virus titers of HSV, compared to the non-treated virus control group ($p < 0.01$), suggesting that myricetin may have direct

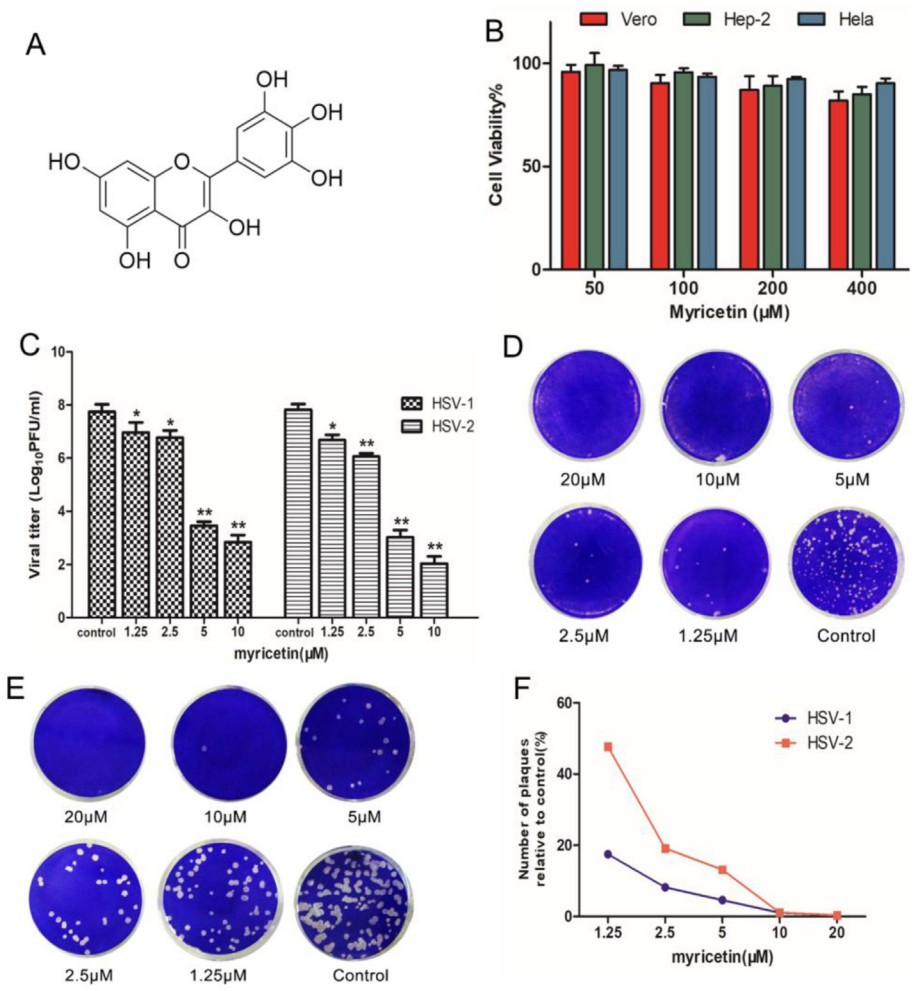

Fig. 1. Inhibitory effects of myricetin on herpes simplex virus *in vitro*. (A) Schematic diagram of the chemical structure of myricetin. (B) The cytotoxicity of myricetin in Vero, Hep-2, HeLa cells was determined by MTT assay after 24 h incubation. The results were presented as a percentage of control group. Values are means ± S.D. (n = 3). (C) The supernatant of HSV (MOI = 1.0) infected cells at 24 h p.i. was collected and the virus yields were determined by plaque assay. Values are means ± S.D. (n = 3). *p < 0.05, **p < 0.01 vs. virus control group. (D and E) Plaque reduction assay of myricetin (1.25, 2.5, 5, 10, 20 μM) pretreated HSV-1 or HSV-2 in Vero cells, respectively. (F) Plaque number from plaque reduction assays performed on Vero cells infected with HSV-1 (D) and HSV-2 (E), the percent inhibition was determined relative to the virus control.

interaction with HSV particles. Treatment of myricetin during adsorption or after adsorption also possessed obvious inhibition on virus multiplication ($p < 0.05$) (Fig. 2A). However, pretreatment of cells did not significantly reduce virus titers *in vitro* (Fig. 2A), suggesting that myricetin may not interact with Vero cells directly. Moreover, the indirect immunofluorescence assay under these four conditions (Pachota et al., 2017) indicated that pretreatment of virus with myricetin (10 μM) before infection also significantly reduced the expression of ICP27 in HSV-1 infected cells (Fig. 2B), which was in concern with the results in plaque assay (Fig. 2A). Thus, myricetin may interact with virus particles to block the adsorption of HSV or inhibit some steps after virus adsorption.

Since myricetin may be able to block adsorption and post-adsorption processes of HSV, we further explored the potential inhibition of myricetin on HSV binding and entry process by using immunofluorescence assay. Briefly, for HSV binding assay, HSV-1 (MOI = 1.0) was adsorbed to HeLa cells for 2 h at 4 °C in the absence or presence of 20 μM myricetin before washing with PBS. For entry assay, HSV-1 (MOI = 1.0) was firstly adsorbed to HeLa cells at 4 °C for 2 h before washing with PBS. Then myricetin (20 μM) was added to cells and incubated at 37 °C for 1 h. After that, cells were treated with proteinase K to remove adsorbed but not internalized virus. Then the immunofluorescence assay was performed to determine the amount of HSV virions binding to or entering into HeLa cells. As shown in Fig. 2C and E, myricetin treatment (20 μM) during adsorption significantly decreased the fluorescence of ICP5 protein on cell surface, compared to

Table 1
Inhibition effects of myricetin and acyclovir on HSV multiplication in different cells.

		CC_{50} (μM)[a]	HSV-1		HSV-2	
			IC_{50} (μM)[b]	SI (CC_{50}/IC_{50})[c]	IC_{50} (μM)[b]	SI (CC_{50}/IC_{50})[c]
Myricetin	Vero	1097.9 ± 71.2	2.2 ± 0.3	498.6	1.6 ± 0.5	685.6
	Hep-2	964.6 ± 94.7	6.3 ± 0.2	153.0	3.5 ± 0.4	275.4
	HeLa	1152.3 ± 165.1	2.5 ± 0.1	460.8	2.1 ± 0.3	548.7
Acyclovir	Vero	975.1 ± 58.1	7.4 ± 0.6	131.8	11.6 ± 2.5	84.1
	Hep-2	897.7 ± 72.6	19.3 ± 2.2	46.5	28.5 ± 4.3	31.5
	HeLa	830.1 ± 40.0	11.0 ± 1.2	75.5	21.9 ± 3.2	37.9

[a] Cytotoxic concentration 50% (CC_{50}): concentration required to reduce cell viability by 50%.
[b] Inhibition concentration 50% (IC_{50}): concentration required to reduce the CPE of the virus by 50% at 24 h p.i.
[c] SI: Selectivity index is defined as the ratio of CC_{50} to IC_{50} (SI = CC_{50}/IC_{50}).

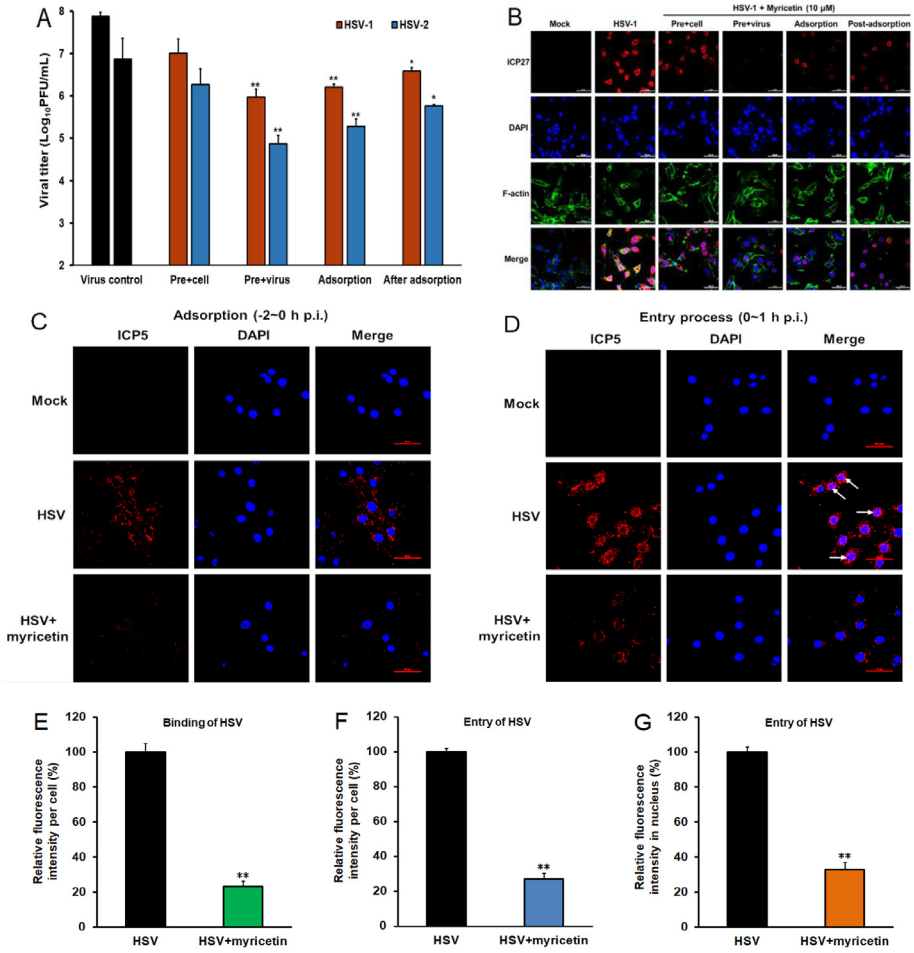

Fig. 2. Influence of different treatment conditions of myricetin on HSV infection. (A) Vero cells were infected with HSV-1 or HSV-2 (MOI = 1.0) using four different treatment conditions. i) Pre + virus: HSV was pretreated with myricetin (20 μM) at 37 °C for 1 h before infection. ii) Pre + cell: Vero cells were pretreated with 20 μM of myricetin before infection. iii) Adsorption: Vero cells were infected in media containing myricetin (20 μM) at 4 °C for 1 h. iv) Post-adsorption: after removal of unabsorbed virus, myricetin (20 μM) was added to the cells. At 24 h p.i., virus yields were determined by plaque assay. The results were presented as mean ± S.D. from five independent experiments. *P < 0.05 vs. virus control group. (B) Vero cells were infected with HSV-1 (F strain) under four treatment conditions of myricetin, and the expression of virus ICP27 protein was detected by immunofluorescence assay. Scale bar represents 50 μm. (C and D) HSV-1 (MOI = 1.0) infected HeLa cells were treated with or without myricetin (20 μM) during adsorption process (C) or entry process (D), then after washing three times with PBS, the immunofluorescence assay was performed by using anti-ICP5 antibody to evaluate the amount of virions binding to or entering into cells. Scale bar represents 50 μm. (E-G) The average fluorescence intensity of ICP5 proteins during adsorption process (E) or entry process (F) was measured by ImageJ (NIH) version 1.33u (USA) to calculate the average intensity per cell of different images (n = 10). The average intensity of ICP5 in cell nucleus during entry process (G) was also measured by ImageJ (USA) to calculate the average intensity per unit area of cell nucleus of different images (n = 10). The average intensity for non-treated virus control cells (HSV) was assigned values of 100 and the data presented as mean ± S.D. (n = 3). Significance: **p < 0.01 vs. virus control group (HSV).

that in non-treated virus control cells, suggesting that myricetin may block virus adsorption process of HSV. Moreover, at 1 h p.i., many fluorescence spot of ICP5 could be found at the nucleus area (white arrow indicated), suggesting that HSV-1 nucleocapsid had been egressed from late endosomes and delivered to the nuclear periphery in HeLa cells (Fig. 2D). However, myricetin treatment during entry process dramatically reduced the fluorescence of ICP5 in cytoplasm, and only very little fluorescence could be observed in cell nucleus, suggesting that myricetin may also be able to block HSV entry process in HeLa cells (Fig. 2D, 2F and 2G). Thus, myricetin may possibly block HSV infection mainly through interfering with HSV binding and entry process.

3.3. Myricetin may interfere with HSV binding and entry process through targeting virus gD protein

Since myricetin may block HSV binding and entry process, we then asked whether myricetin could inhibit the virus-induced membrane fusion process. As shown in Fig. 3A, in HSV-2 (MOI = 3.0) infected Vero cells, obvious syncytia with multinuclear cells were observed in non-treated virus control group (HSV-2) at 7 h p.i. However, treatment with myricetin (30, 15 μM) during 5–7 h p.i. markedly blocked syncytium formation only with a limited number of small syncytia, suggesting that myricetin may inhibit HSV-induced cell fusion. In addition, myricetin treatment during 5–7 h p.i. did not obviously influence the expression of virus surface glycoproteins such as gD protein (Fig. 3B). Thus, myricetin may directly block HSV-induced membrane fusion through inhibiting the function of virus surface glycoproteins rather than reducing their expression.

Since myricetin can inhibit both HSV adsorption and membrane fusion, we then questioned whether myricetin directly interacts with virus surface gD protein which is mainly required for HSV entry process. We employed a drug affinity responsive target stability assay (DARTS) (Lomenick et al., 2009), which relies on the reduction of protease susceptibility of the target protein upon drug binding, to detect the potential interaction between myricetin and gD protein. In brief, HSV-1 infected Vero cell lysates were digested with pronase in the presence or absence of myricetin (60 μM), then the amount of gD protein in cell lysates was detected by western blotting. As shown in Fig. 3C, HSV-1 gD protein was obviously protected by protease digestion in the extracts of myricetin (60 μM) treated cells especially under pronase treatment at 3 μg/ml, suggesting that myricetin may interact with HSV gD protein in HSV-1 infected Vero cells. However, myricetin (60 μM) could not protect other virus surface glycoproteins such as gB, gC, and gH/gL proteins from protease digestion in HSV-1 infected cells (Fig. 3D). Similarly, the cellular surface receptors of HSV-1 such as HVEM and nectin-1 could also not be protected from protease digestion by myricetin (60 μM) (Fig. 3D). Thus, myricetin may interfere with HSV binding and entry process through targeting virus gD protein rather than cellular receptors of HSV.

Moreover, the direct interaction between myricetin and gD protein was further evaluated by using SPR assay (Geng et al., 2003). Briefly, with HSV-1 gD proteins being immobilized on the chip, myricetin at the concentrations of 0.3125–10 μM was flowed over the biosensor chip surface, respectively. Data revealed a marked binding of myricetin to virus gD protein in a concentration-dependent manner with a KD equivalent to about 6.088E-8 M (60.88 nM), implicating a high affinity of myricetin for HSV-1 gD protein (Fig. 3E). Thus, pretreatment of HSV

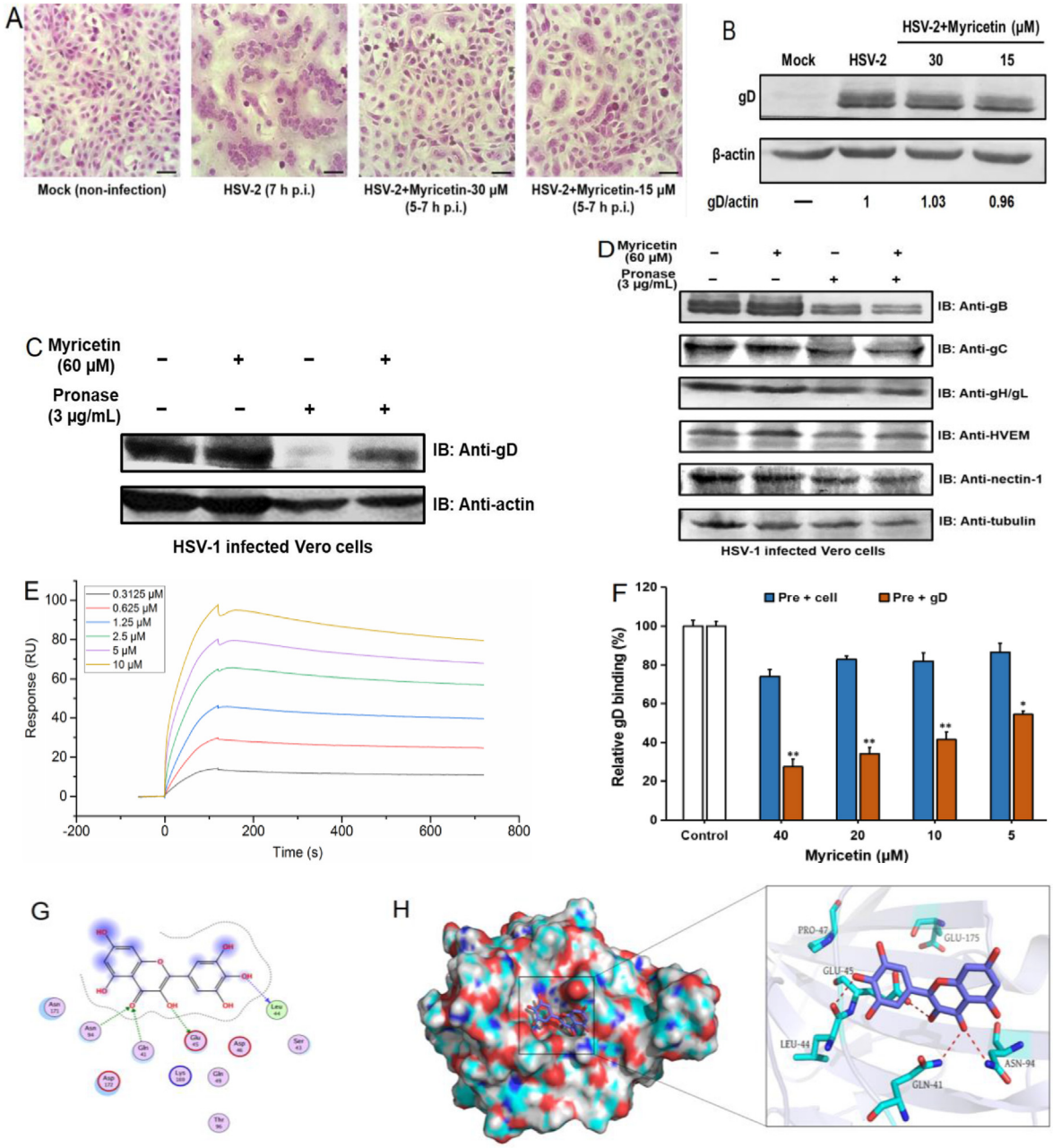

Fig. 3. Myricetin may interfere with HSV infection through targeting virus gD protein. (A) HSV-2 (MOI = 3.0) infected Vero cells were added with or without myricetin (30, 15 μM) at 5 h post infection (p.i.), and incubated at 37 ˚C for 2 h. Then the cells were fixed and stained with HE solution. The inhibition of syncytium formation of HSV-2 was observed using optical microscopy. Bar represents 50 μm. (B) The influence of myricetin on virus gD expression during 5–7 h p.i. was evaluated by western blotting. (C and D) DARTS analysis for myricetin. HSV-1 infected Vero cell lysates were incubated with or without myricetin (60 μM) for 1 h and then digested with pronase (3 μg/ml) for 30 min. Protein samples were separated by SDS-PAGE and immunoblotted with the indicated antibodies against virus gD, gB, gC, gH/gL proteins or cellular HVEM, nectin-1, actin or tubulin proteins. The results shown are representative of three independent experiments. (E) The HSV-1 gD proteins were firstly immobilized onto the surface of a carboxymethylated dextran sensor chip (CM5). To assess realtime binding of myricetin to the gD proteins on CM5 chips, myricetin (10, 5, 2.5, 1.25, 0.625, 0.3125 μM) was flowed over the biosensor chip surface. The sensorgram for all binding interactions were recorded in real time and were analysed after subtracting the sensorgram from the blank channel. Then, the changes in mass due to the binding response were recorded as resonance units (RU). (F) HSV-1 gD binding assay. Vero cells were first treated with or without myricetin (40, 20, 10, 5 μM) for 1 h, then the HSV-1 gD protein or myricetin (40, 20, 10, 5 μM) pretreated gD protein (2 μg/mL) were added to cells and incubated for another 1 h, respectively. Then the amount of gD protein binding to Vero cell surface was detected by ELISA assay using anti-gD antibody and HRP labeled secondary antibody sequentially. Values are means ± SD (n = 3). Significance: **p < 0.01 vs. virus control group. (G and H) The 2D (G) and 3D (H) binding mode of myricetin with HSV gD protein (PDB ID: 4MYV) was shown. Myricetin is colored in purple, the surrounding residues in the binding pockets are colored in cyan. The backbone of the receptor is depicted as lightblue cartoon. (For interpretation of the references to color in this figure legend, the reader is referred to the Web version of this article.)

with myricetin before infection may allow myricetin to fully bind gD protein and form a stable myricetin-gD complex.

Furthermore, the impact of myricetin on HSV-1 gD binding to Vero cells was further explored using a cell enzyme-linked immunosorbent assay, as previously described (Tiwari et al., 2006). Briefly, Vero cells were first treated with or without myricetin (40, 20, 10, 5 μM) for 1 h, then the HSV-1 gD protein or myricetin (40, 20, 10, 5 μM) pretreated gD protein (2 μg/mL) were added to cells and incubated for another 1 h,

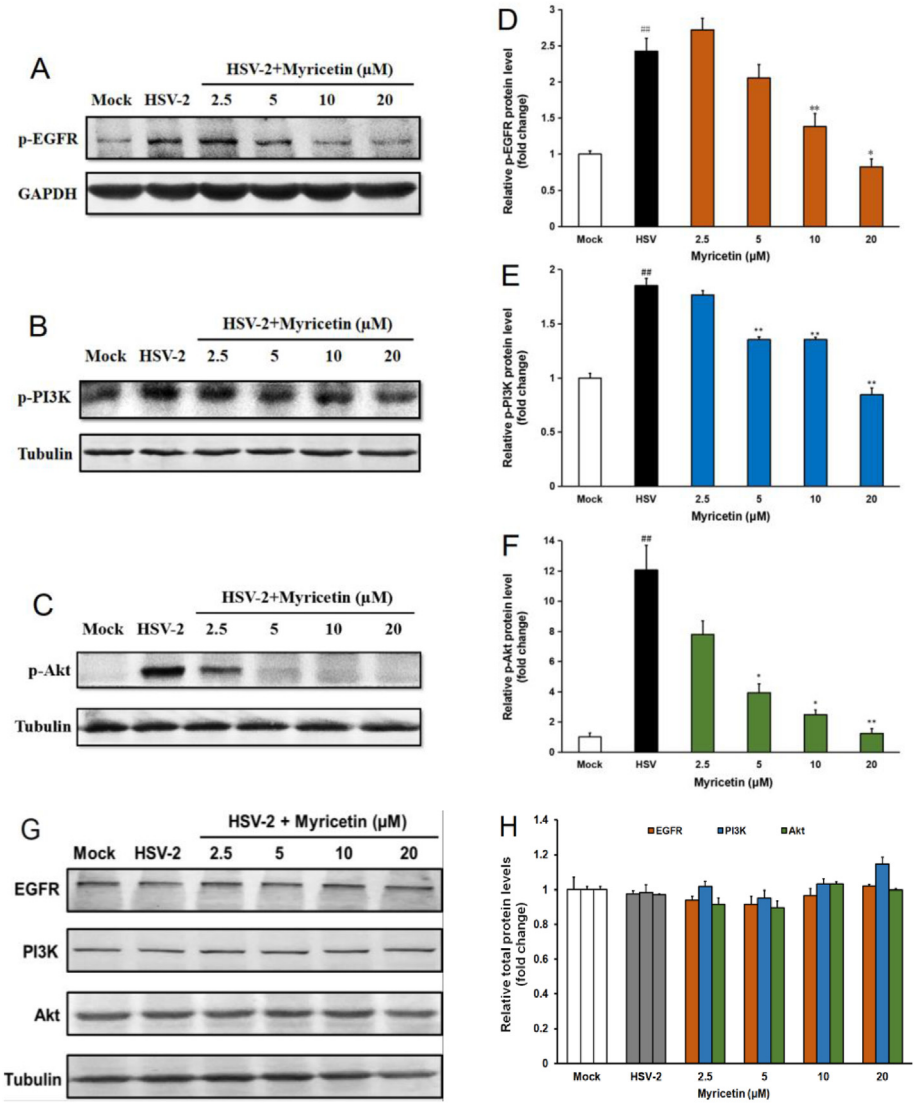

Fig. 4. Involvement of EGFR/PI3K/Akt signaling pathway in the anti-HSV actions of myricetin. (A-C) HSV-2 (MOI = 1.0) infected cells were treated with or without myricetin (2.5, 5, 10, 20 μM) for 2 h, and then the phosphorylation of EGFR (A), PI3K (B), and Akt (C) was evaluated by western blot. Blots were also probed for GAPDH and α-tubulin proteins as loading controls. The result shown is a representative of three separate experiments. (D-F) Quantification of immunoblot for the ratio of p-EGFR (D), p-PI3K (E), p-Akt (F) protein to GAPDH or tubulin, respectively. The ratio for non-infected cells (M) was assigned values of 1.0 and the data presented as mean ± S.D. (n = 3). Significance: ##p < 0.01 vs. normal control group (Mock); *p < 0.05, **p < 0.01 vs. virus control group (HSV). (G) HSV-2 (MOI = 1.0) infected cells were treated with or without myricetin (2.5, 5, 10, 20 μM) for 2 h, and then the total expression levels of EGFR, PI3K, and Akt were evaluated by western blot. The result shown is a representative of three separate experiments. (H) Quantification of immunoblot for the ratio of EGFR, PI3K, Akt protein to α-tubulin, respectively. The ratio for non-infected cells (Mock) was assigned values of 1.0 and the data presented as mean ± S.D. (n = 3).

respectively. Then the amount of gD protein binding to Vero cell surface was detected by sequentially incubated with anti-gD antibody and HRP labeled secondary antibody. As shown in Fig. 3F, pre-incubation of gD protein with myricetin (5, 10, 20, 40 μM) significantly reduced the binding of gD to cell surface in a dose-dependent manner, however, pretreatment of cells did not significantly decrease the amount of gD protein on cell surface. This finding strongly supports that myricetin may interact with HSV gD protein rather than cellular receptors to block virus binding and entry.

To further investigate the binding mode of myricetin with gD, docking simulation studies were carried out using the crystal structure of HSV-1 gD protein (PDB code: 4MYV). The results indicated that the oxygen atom of carbanyl group of myricetin, regarded as hydrogen bond acceptor, forms two hydrogen bonds with the nitrogen atom of amide group of Gln41 as well as Asn94 in gD (Fig. 3G). The oxygen atom of phenolic hydroxyl group of myricetin, regarded as hydrogen bond donor, forms a hydrogen bond with the oxygen atom of backbone of Leu44 in gD. The oxygen atom of hydroxyl group of myricetin, regarded as hydrogen bond donor, forms a hydrogen bond with the oxygen atom of carboxyl group of Glu45 in gD (Fig. 3G and H). Thus, myricetin may interact with Gln41, Leu44, Glu45 and Asn94 of gD through hydrogen bond interactions.

3.4. Cellular EGFR/PI3K/Akt signaling pathway may be involved in the anti-HSV actions of myricetin

Since myricetin may inhibit HSV entry process in HeLa cells, we further explored whether myricetin could influence the HSV infection-related signaling pathways by using western blot assay. The EGFR/PI3K/Akt signaling pathway was reported to be required for virus endocytosis and replication, and the inhibitors of PI3K signaling could inhibit both entry and fusion of HSV (Eierhoff et al., 2010; Tiwari and Shukla, 2010). Herein, treatment with myricetin (10, 20 μM) for 2 h significantly decreased the levels of phosphorylated EGFR from about 2.4 to about 1.4 and 0.8-fold of normal control group, respectively ($p < 0.05$) (Fig. 4A and D). Moreover, the activation of downstream signal PI3K was also evaluated, and the results showed that treatment with myricetin (5, 10, 20 μM) for 2 h significantly decreased the levels of phosphorylated PI3K proteins from about 1.9 to about 1.4, 1.4, and 0.8-fold of normal control group, respectively ($p < 0.01$) (Fig. 4B and E). In addition, treatment with myricetin (5, 10, 20 μM) for 2 h significantly reduced the activation of Akt from about 12.1 to about 3.9, 2.5, and 1.2-fold of normal control group, respectively ($p < 0.05$) (Fig. 4C and F). However, myricetin (2.5, 5, 10, 20 μM) treatment did not significantly influence the total expression levels of EGFR, PI3K and Akt proteins in HSV-2 infected Vero cells (Fig. 4G and H). Thus, cellular EGFR/PI3K/Akt signaling pathway may be involved in the anti-HSV

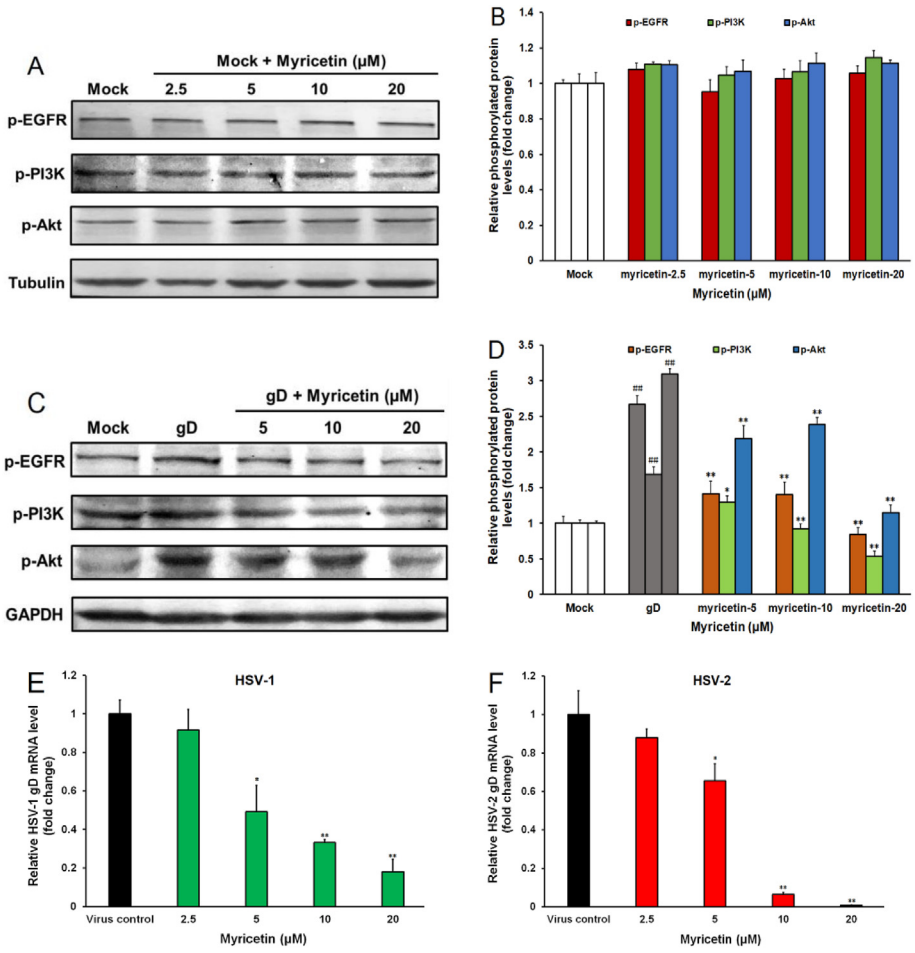

Fig. 5. The inhibition of EGFR/PI3K/Akt pathway by myricetin may be related to its inhibition of gD protein. (A) Non-infected Vero cells were treated with or without myricetin (2.5, 5, 10, 20 μM) for 2 h, and then the phosphorylation of EGFR, PI3K, and Akt was evaluated by western blot. Blots were also probed for α-tubulin proteins as loading controls. The result shown is a representative of three separate experiments. (B) Plots quantifying the immunoblots (as ratios to tubulin) for p-EGFR, p-PI3K and p-Akt proteins. The ratios for non-treated cells (Mock) were assigned values of 1.0 and the data presented as mean ± S.D. (n = 3). (C) Vero cells were treated with or without gD proteins in the presene or absence of myricetin (5, 10, 20 μM) for 2 h, and then the phosphorylation of EGFR, PI3K, and Akt was evaluated by western blot. Blots were also probed for GAPDH proteins as loading controls. The result shown is a representative of three separate experiments. (D) Quantification of immunoblot for the ratio of p-EGFR, p-PI3K, p-Akt protein to GAPDH, respectively. The ratio for non-treated control cells (Mock) was assigned values of 1.0 and the data presented as mean ± S.D. (n = 3). Significance: ##p < 0.01 vs. normal control group (Mock); *p < 0.05, **p < 0.01 vs. gD treated control group (gD). (E and F) HSV (MOI = 1.0) infected Vero cells were treated with myricetin (2.5, 5, 10, 20 μM), and incubated at 37 °C for 8 h. After that, total RNA was extracted for real-time RT-PCR assay of HSV-1 (E) and HSV-2 (F) gD mRNAs and cellular β-actin mRNA. The relative amounts of HSV gD mRNAs were determined using the comparative ($2^{-\Delta\Delta CT}$) method. RNA levels for non-treated virus control cells (HSV) were assigned values of 1.0. Values are means ± SD (n = 3). Significance: *p < 0.05, **p < 0.01 vs. virus control group.

actions of myricetin *in vitro*.

Furthermore, myricetin (2.5, 5, 10, 20 μM) treatment could not significantly influence the activation of EGFR, PI3K and Akt proteins in the non-infected Vero cells (Fig. 5A and B), suggesting that the inhibition of EGFR/PI3K/Akt pathway by myricetin may be related to its inhibition of HSV infection. Moreover, treatment with HSV-1 gD protein (2 μg/ml) could significantly enhance the phosphorylation of EGFR, PI3K, and Akt proteins in the non-infected Vero cells ($p < 0.01$), suggesting that the activation of EGFR/PI3K/Akt pathway in HSV infected cells may be related to the binding of gD to cellular receptors (Fig. 5C and D). However, after myricetin treatment (5, 10, 20 μM), the levels of phosphorylated EGFR, PI3K, and Akt proteins were significantly reduced as compared to the gD treated control group ($p < 0.05$) (Fig. 5C and D). In addition, myricetin treatment (5, 10, 20 μM) also significantly reduced the expression level of gD mRNA in HSV-1 and HSV-2 infected Vero cells ($p < 0.05$) (Fig. 5E and F). Considered that EGFR/PI3K/Akt pathway is required for efficient HSV replication, we suppose that myricetin may be able interact with virus gD protein to interfere with the activation of EGFR/PI3K/Akt pathway to further inhibit subsequent replication of HSV.

3.5. Myricetin also possessed in vivo antiviral activity in HSV-1 infected mice

The anti-HSV effects of myricetin were further tested in a murine intranasal model of HSV pneumonia and encephalitis (De Clercq and Luczak, 1976). In brief, HSV-1 (F strain)-infected mice received intraperitoneal treatment of myricetin (2.5 or 5 mg·kg-1), acyclovir (10 mg·kg-1), or placebo (PBS) once daily for five days. As shown in Fig. 6A, intraperitoneal treatment of myricetin (2.5 or 5 mg·kg-1) significantly increased survival rates as compared to the placebo-treated control group ($p < 0.01$). By day 14 post infection, only 20% of the individuals in the placebo group survived whereas 100% of animals in the myricetin-treated group survived, superior to that in acyclovir (10 mg·kg-1)-treated group (90%). Moreover, the body weights of mice in virus control group (Placebo) began to decrease at 6 days p.i., losing up to 19% of initial weight, before gradually recovering. However, myricetin (2.5 or 5 mg·kg-1)-treated mice gradually increased their body weights only with a limited weight loss of less than 5% during the infection, superior to those in the acyclovir (10 mg·kg-1) treated group (Fig. 6B).

Furthermore, four days post-infection, four mice of each treatment group were sacrificed and the tissue samples were removed for further analysis. Subsequently, the viral titers in the lung and spinal cord were determined by plaque assay and quantitative RT-PCR. The results showed that after treatment of myricetin for four days, the pulmonary virus titers significantly decreased compared to that of the virus control group ($p < 0.05$) (Fig. 6C). The relative virus gD mRNA levels in spinal cord also significantly reduced compared to that of the placebo group, suggesting that intraperitoneal therapy with myricetin could inhibit HSV multiplication in mice (Fig. 6D). Acyclovir (10 mg·kg-1) treatment also showed significant reduction of virus titers in mice lungs and spinal cord (Fig. 6C and D).

To further evaluate the effects of myricetin on viral pneumonia and encephalitis in mice, histopathology analysis was also performed. The results showed that the lung tissues in virus-control group showed marked infiltration of inflammatory cells and the presence of massive hyperaemia in the lumen (Fig. 6E). However, mice treated with myricetin (2.5 or 5 mg·kg-1) following infection had intact columnar epithelium even in the presence of tiny serocellular exudates in the lumen

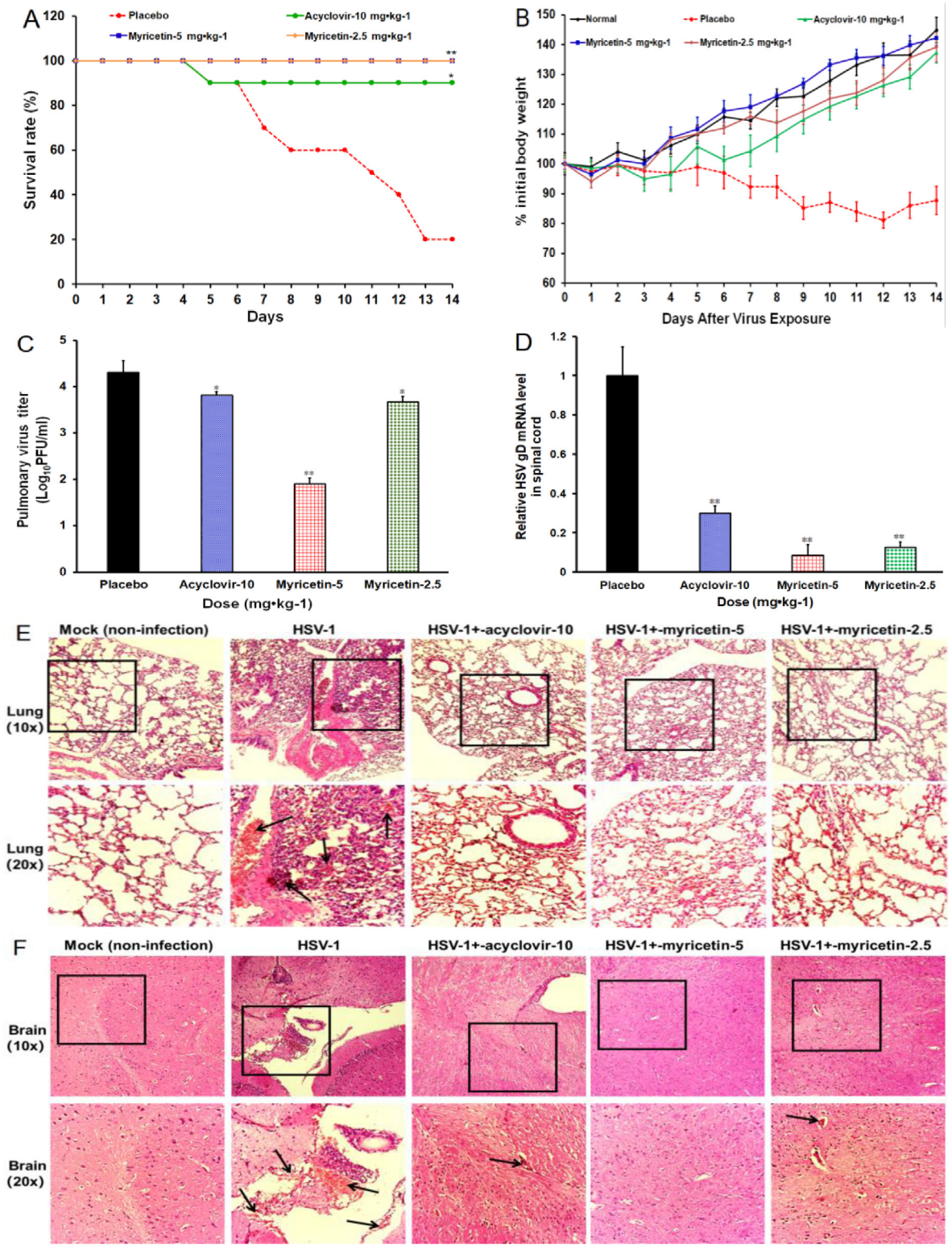

Fig. 6. The anti-HSV actions of myricetin *in vivo*. (A) Survival rate. HSV-1 infected mice were received intraperitoneally treatment of myricetin (2.5 or 5 mg·kg-1), acyclovir (10 mg·kg-1), or placebo (PBS) once daily for five days. Results are expressed as percentage of survival, evaluated daily for 14 days. Significance: *p < 0.05, **p < 0.01 vs. virus control group (placebo). (B) HSV infected mice were received intraperitoneally treatment with indicated compounds for five days. The average body weights in each group were monitored daily for 14 days and are expressed as a percentage of the initial value. (C and D) Viral titers in lungs and spinal cord. After intraperitoneal therapy with indicated compounds for five days, the viral titers in lungs (C) and spinal cords (D) were evaluated by plaque assay and quantitative RT-PCR assay on day 4 p.i., respectively. Values are means ± S.D. (n = 4). Significance: *p < 0.05, **p < 0.01 vs. virus control group. (E and F) Histopathology analyses of lung and brain tissues on Day 4 p.i. by HE staining (× 10 and × 20). The representative micrographs from each group were shown. Mock: non-infected mice tissues; HSV-1: HSV-1 infected tissues without drugs; HSV-1 + acyclovir-10: HSV-1 infected tissues with acyclovir (10 mg·kg-1) treatment; HSV-1 + myricetin-5: HSV-1 infected tissues with myricetin (5 mg·kg-1) treatment; HSV-1 + myricetin-2.5: HSV-1 infected tissues with myricetin (2.5 mg·kg-1) treatment; The black arrows indicate the presence of hyperaemia and infiltration of inflammatory cells in the lumen.

(Fig. 6E). In addition, treatment of myricetin (5 mg·kg-1) nearly had no hyperaemia and infiltration of inflammatory cells in brain tissues (Fig. 6F). Myricetin (2.5 mg·kg-1) treated mice only had tiny hyperaemia in the brain tissues, comparable to the effects of acyclovir (10 mg·kg-1) (Fig. 6F). Thus, myricetin may be able to attenuate pneumonia and encephalitis symptoms in HSV infected mice.

4. Discussion

Myricetin is a member of the flavonoid class of polyphenolic compounds, which was reported to possess antiviral activities against lots of viruses including HIV and SARS-CoV (Ong and Khoo, 1997). In this study, we discovered that myricetin possessed anti-HSV-1 and HSV-2 activities in different cells with very low toxicity (SI $>$ 150). Myricetin may block HSV infection through direct interaction with virus gD protein to interfere with virus adsorption and membrane fusion, which was different from the nucleoside analogues such as acyclovir. Most importantly, intraperitoneal therapy of HSV-1-infected mice with myricetin markedly improved their survival and reduced virus titers in both lungs and spinal cord.

Pretreatment of HSV by myricetin before infection significantly reduced the virus titers in HSV infected cells, suggesting that myricetin may have direct interaction with HSV particles. In addition, myricetin can block HSV induced membrane fusion and interfere with virus binding and entry process, suggesting that myricetin may interact with some surface glycoproteins of HSV. The results of DARTS assay and gD binding assay indicated that myricetin may interact with virus gD protein rather than cellular receptors of HSV to block virus binding and entry (Fig. 3). The data from SPR assay verified that myricetin can truly bind to HSV-1 gD protein with high affinity (KD $\approx$ 60.88 nM) (Fig. 3E). The molecular docking analysis indicated that myricetin may interact with Gln41, Leu44, Glu45 and Asn94 of gD protein through hydrogen bond interactions (Fig. 3G and H). Furthermore, myricetin treatment inhibited the activation of EGFR, PI3K and Akt proteins in HSV infected or gD treated non-infected cells, and reduced the mRNA levels of virus proteins in HSV-infected cells (Fig. 5). Considered that EGFR/PI3K/Akt pathway is required for efficient HSV replication (Tiwari and Shukla, 2010), we suppose that myricetin may interact with virus gD protein to interfere with the activation of EGFR/PI3K/Akt pathway so as to further inhibit subsequent replication of HSV.

The mouse model of HSV intranasal infection has been used for studying HSV induced pneumonia and encephalitis (Gamba et al., 2004). In this study, intraperitoneal therapy of HSV-1-infected mice with myricetin markedly improved their survival and inhibited HSV multiplication in both lungs and spinal cord (Fig. 6). Moreover, the histopathological analysis indicated that myricetin treatment also significantly attenuated the pneumonia and encephalitis symptoms in HSV-infected mice, comparable to the effects of acyclovir. In contrast to acyclovir, myricetin can block HSV binding and entry process with low toxicity, suggesting that it may be used for therapy and prophylaxis of HSV infection. However, oral administration of myricetin as an antiviral may be unlikely to be successful because of its rapid metabolism. Thus, myricetin may be used for prevention and treatment of herpes simplex pneumonia and encephalitis by intravenous administration in the future.

In summary, myricetin possessed anti-HSV activities both *in vitro* and *in vivo* with low toxicity. Myricetin may block HSV infection through direct interaction with virus gD protein to interfering with virus adsorption and membrane fusion. In addition, cellular EGFR/PI3K/Akt pathway was also involved in the anti-HSV actions of myricetin. Thus, myricetin merits further investigation as a novel anti-HSV agent targeting both virus gD protein and host EGFR/PI3K/Akt pathway. Further studies of the anti-HSV effects of myricetin against clinical strains especially the acyclovir-resistant strains will be required to advance it for drug development. Nevertheless, myricetin has the potential to be developed into a novel antiviral injection for therapy of herpes simplex encephalitis and pneumonia in the future.

Declaration of competing interest

None declared.

Acknowledgements

This work was supported by National Natural Science Foundation of China (81874320, 81741146, 31500646), NSFC-Shandong Joint Fund (U1606403, U1706210), Shandong Provincial Natural Science Foundation (ZR2017MH013), and Qingdao Marine Biomedical Science and Technology Innovation Center (2017-CXZX01-3-11).

Appendix A. Supplementary data

Supplementary data to this article can be found online at https://doi.org/10.1016/j.antiviral.2020.104714.

References

Carr, D.J., Harle, P., Gebhardt, B.M., 2001. The immune response to ocular herpes simplex virus type 1 infection. Exp. Biol. Med. 226, 353–366.
Cushnie, T.P., Lamb, A.J., 2005. Antimicrobial activity of flavonoids. Int. J. Antimicrob. Agents 26, 343–356.
Dai, W., Wu, Y., Bi, J., Wang, S., Li, F., Kong, W., Barbier, J., Cintrat, J.C., Gao, F., Gillet, D., Su, W., Jiang, C., 2018. Antiviral effects of ABMA against herpes simplex virus type 2 in vitro and in vivo. Viruses 10.
Dajas, F., Rivera-Megret, F., Blasina, F., Arredondo, F., Abin-Carriquiry, J.A., Costa, G., Echeverry, C., Lafon, L., Heizen, H., Ferreira, M., Morquio, A., 2003. Neuroprotection by flavonoids. Braz. J. Med. Biol. Res. 36, 1613–1620.
De Clercq, E., Luczak, M., 1976. Intranasal challenge of mice with herpes simplex virus: an experimental model for evaluation of the efficacy of antiviral drugs. J. Infect. Dis. 133 (Suppl_2), A226–A236.
Du, R., Wang, L., Xu, H., Wang, Z., Zhang, T., Wang, M., Ning, Y., Deng, F., Hu, Z., Wang, H., Li, Y., 2017. A novel glycoprotein D-specific monoclonal antibody neutralizes herpes simplex virus. Antivir. Res. 147, 131–141.
Eierhoff, T., Hrincius, E.R., Rescher, U., Ludwig, S., Ehrhardt, C., 2010. The epidermal growth factor receptor (EGFR) promotes uptake of influenza A viruses (IAV) into host cells. PLoS Pathog. 6, e1001099.
Fatahzadeh, M., Schwartz, R.A., 2007. Human herpes simplex virus infections: epidemiology, pathogenesis, symptomatology, diagnosis, and management. J. Am. Acad. Dermatol. 57, 737–763.
Gamba, G., Cavalieri, H., Courreges, M.C., Massouh, E.J., Benencia, F., 2004. Early inhibition of nitric oxide production increases HSV-1 intranasal infection. J. Med. Virol. 73, 313–322.
Geng, M.Y., Li, F.C., Xin, X.L., Li, J., Yan, Z.W., Guan, H.S., 2003. The potential molecular targets of marine sulfated polymannuroguluronate interfering with HIV-1 entry: interaction between SPMG and HIV-1 rgp120 and CD4 molecule. Antivir. Res. 59, 127–135.
Gupta, S.C., Tyagi, A.K., Deshmukh-Taskar, P., Hinojosa, M., Prasad, S., Aggarwal, B.B., 2014. Downregulation of tumor necrosis factor and other proinflammatory biomarkers by polyphenols. Arch. Biochem. Biophys. 559, 91–99.
Li, M.K., Liu, Y.Y., Wei, F., Shen, M.X., Zhong, Y., Li, S., Chen, L.J., Ma, N., Liu, B.Y., Mao, Y.D., Li, N., Hou, W., Xiong, H.R., Yang, Z.Q., 2018. Antiviral activity of arbidol hydrochloride against herpes simplex virus I in vitro and in vivo. Int. J. Antimicrob. Agents 51, 98–106.
Li, T., Liu, L., Wu, H., Chen, S., Zhu, Q., Gao, H., Yu, X., Wang, Y., Su, W., Yao, X., Peng, T., 2017. Anti-herpes simplex virus type 1 activity of Houttuynoid A, a flavonoid from Houttuynia cordata Thunb. Antivir. Res. 144, 273–280.
Liu, X., Cohen, J.I., 2015. The role of PI3K/Akt in human herpesvirus infection: from the bench to the bedside. Virology 479–480, 568–577.
Livak, K.J., Schmittgen, T.D., 2001. Analysis of relative gene expression data using real-time quantitative PCR and the 2(-Delta Delta C(T)) method. Methods 25, 402–408.
Lomenick, B., Hao, R., Jonai, N., Chin, R.M., Aghajan, M., Warburton, S., Wang, J., Wu, R.P., Gomez, F., Loo, J.A., Wohlschlegel, J.A., Vondriska, T.M., Pelletier, J., Herschman, H.R., Clardy, J., Clarke, C.F., Huang, J., 2009. Target identification using drug affinity responsive target stability (DARTS). Proc. Natl. Acad. Sci. U.S.A. 106, 21984–21989.
Lyu, S.Y., Rhim, J.Y., Park, W.B., 2005. Antiherpetic activities of flavonoids against herpes simplex virus type 1 (HSV-1) and type 2 (HSV-2) in vitro. Arch Pharm. Res. (Seoul) 28 (11), 1293–1301.
Molecular Operating Environment (MOE), M., 2014. Chemical Computing Group Inc.: 1010 Sherbooke St. West, Suite #910, Montreal, QC, Canada, H3A 2R7.
Morfin, F., Thouvenot, D., 2003. Herpes simplex virus resistance to antiviral drugs. J. Clin. Virol. 26, 29–37.
Ong, K.C., Khoo, H.E., 1997. Biological effects of myricetin. Gen. Pharmacol. 29, 121–126.
Pachota, M., Klysik, K., Synowiec, A., Ciejka, J., Szczubialka, K., Pyrc, K., Nowakowska,

M., 2017. Inhibition of herpes simplex viruses by cationic dextran derivatives. J. Med. Chem. 60, 8620–8630.
Pasetto, S., Pardi, V., Murata, R.M., 2014. Anti-HIV-1 activity of flavonoid myricetin on HIV-1 infection in a dual-chamber in vitro model. PloS One 9, e115323.
Ross, J.A., Kasum, C.M., 2002. Dietary flavonoids: bioavailability, metabolic effects, and safety. Annu. Rev. Nutr. 22, 19–34.
Santhakumar, A.B., Bulmer, A.C., Singh, I., 2014. A review of the mechanisms and effectiveness of dietary polyphenols in reducing oxidative stress and thrombotic risk. J. Hum. Nutr. Diet. 27, 1–21.
Semwal, D.K., Semwal, R.B., Combrinck, S., Viljoen, A., 2016. Myricetin: a dietary molecule with diverse biological activities. Nutrients 8, 90.
Smith, J.S., Robinson, N.J., 2002. Age-specific prevalence of infection with herpes simplex virus types 2 and 1: a global review. J. Infect. Dis. 186 (Suppl. 1), S3–S28.
Tian, L.W., Zhang, Y.J., Qu, C., Wang, Y.F., Yang, C.R., 2010. Phloroglucinol glycosides from the fresh fruits of Eucalyptus maideni. J. Nat. Prod. 73, 160–163.
Tiwari, V., Clement, C., Xu, D., Valyi-Nagy, T., Yue, B.Y., Liu, J., Shukla, D., 2006. Role for 3-O-sulfated heparan sulfate as the receptor for herpes simplex virus type 1 entry into primary human corneal fibroblasts. J. Virol. 80 (18), 8970–8980.
Tiwari, V., Shukla, D., 2010. Phosphoinositide 3 kinase signalling may affect multiple steps during herpes simplex virus type-1 entry. J. Gen. Virol. 91, 3002–3009.
Wang, W., Yin, R.J., Zhang, M., Yu, R.L., Hao, C., Zhang, L.J., Jiang, T., 2017. Boronic acid modifications enhance the anti-influenza A virus activities of novel quindoline derivatives. J. Med. Chem. 60, 2840–2852.
Yu, M.S., Lee, J., Lee, J.M., Kim, Y., Chin, Y.W., Jee, J.G., Keum, Y.S., Jeong, Y.J., 2012. Identification of myricetin and scutellarein as novel chemical inhibitors of the SARS coronavirus helicase, nsP13. Bioorg. Med. Chem. Lett 22, 4049–4054.